

Highly Reduced Fine-Structure Splitting in InAs/InP Quantum Dots Offering an Efficient On-Demand Entangled 1.55- μm Photon Emitter

Lixin He,^{1,*} Ming Gong,¹ Chuan-Feng Li,¹ Guang-Can Guo,¹ and Alex Zunger²

¹Key Laboratory of Quantum Information, University of Science and Technology of China, Hefei, 230026, People's Republic of China

²National Renewable Energy Laboratory, Golden, Colorado 80401, USA

(Received 2 June 2008; published 9 October 2008)

To generate entangled photon pairs via quantum dots (QDs), the exciton fine-structure splitting (FSS) must be comparable to the exciton homogeneous linewidth. Yet in the (In, Ga)As/GaAs QD, the intrinsic FSS is about a few tens μeV . To achieve photon entanglement, it is necessary to cherry-pick a sample with extremely small FSS from a large number of samples or to apply a strong in-plane magnetic field. Using theoretical modeling of the fundamental causes of FSS in QDs, we predict that the intrinsic FSS of InAs/InP QDs is an order of magnitude smaller than that of InAs/GaAs dots, and, better yet, their excitonic gap matches the 1.55 μm fiber optic wavelength and, therefore, offers efficient on-demand entangled photon emitters for long distance quantum communication.

DOI: 10.1103/PhysRevLett.101.157405

PACS numbers: 78.67.Hc, 42.50.-p, 73.21.La

Entangled photon pairs distinguished themselves from the classically correlated photons because of their non-locality [1,2] and therefore play a crucial role in quantum information applications, including quantum teleportation [3], quantum cryptography [4], and distributed quantum computation [5]. Benson *et al.* [6] proposed that a biexciton cascade process in a self-assembled quantum dot (QD) can be used to generate the “event-ready” entangled photon pairs, with orders of magnitude higher efficiency than the traditional parametric down-conversion method [2–4]. This process is shown schematically in Fig. 1(a), in which a biexciton decays into two photons via two paths of different polarizations $|H\rangle$ and $|V\rangle$. If the two paths are indistinguishable, the final result is a polarization entangled photon pair state [6,7] $(|H_{xx}H_x\rangle + |V_{xx}V_x\rangle)/\sqrt{2}$. However, early attempts [6] to generate the entangled photon pairs using the InAs/GaAs QDs were unsuccessful, because the $|H\rangle$ - and $|V\rangle$ -polarized photons have a small energy difference due to the asymmetric electron-hole exchange interaction in the QDs [see Fig. 1(b)]. The small energy splitting, known as the fine-structure splitting (FSS), is typically about -40 to $+80$ μeV in the InAs/GaAs QDs [8–10], which is much larger than the radiative linewidth (~ 1.0 μeV) [7,11]. Such a splitting provides therefore “which way” information about the photon decay path that can destroy the photon entanglement, leaving only classically correlated photon pairs [7,11].

To achieve photon entanglement, the FSS must be reduced to a value comparable to the exciton homogeneous linewidth. The lack of a detailed understanding of the factors controlling FSS in QDs has thus far impeded the design of small FSS values in quantum systems. It was, however, empirically discovered that the FSS in InAs/GaAs QDs can be significantly reduced or even reversed by various thermal annealing protocols [8,10,12]. Furthermore, in alloy dots of (In, Ga)As/GaAs, different random

realizations of Ga and In distributions on the cation lattice lead a distribution of FSS values. Careful screening of dots out of a large ensemble can then be used to [7] find those with small FSS. By applying such “cherry-picking” techniques, entangled photon pairs have been recently achieved in the (In, Ga)As/GaAs QDs [7]. However, even after thermal annealing, the FSS is still about ± 10 μeV , too large for generating entangled photon pairs [7]. The FSS can be further reduced by applying an in-plane magnetic field [7], which, however, significantly complicates the experimental setup. Furthermore, after thermal annealing, the exciton wavelength is reduced to 880–950 nm, becoming uncomfortably close to the energy of the wetting layer emission, thus leading to unwanted strong background light [7,13], and the wavelength is also too short for the optical fiber communications.

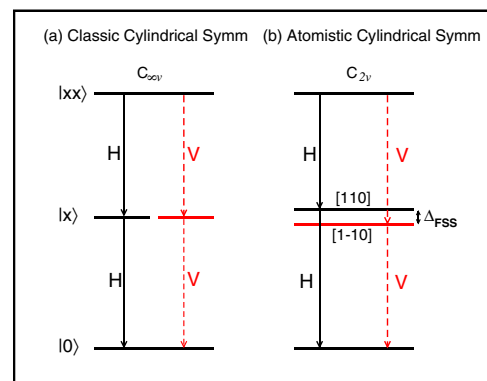


FIG. 1 (color online). (a) A schematic illustration of the biexciton cascade process to generate polarization entangled photons in a QD with classic cylindrical symmetry. (b) Because of the in-plane asymmetry, the H - and V -polarized photons have a small energy splitting Δ_{FSS} , which may destroy the polarization entanglement.

The reason for the early optimism about the use of QD for generating entangled photon pairs stems from the thought that FSS of an exciton will vanish [see Fig. 1(a)] in shape-symmetric (e.g., cylindrical) dots [14]. However, the FSS of an exciton in a dot contains two terms: the previously largely ignored “intrinsic FSS” [14], which is nonzero even in a shaped-symmetric dot, and the “shape-asymmetric FSS” due to deviation from geometric symmetry along the [110] and $[1\bar{1}0]$ directions [12]. In this sense, the FSS is just like the spin-splitting effects, which are composed of the intrinsic Dresselhaus term [15], due to the bulk inversion asymmetry, and the Rashba term [16], due to the geometrical asymmetry. Whereas the contribution to the FSS of QD shape asymmetry [12] can be reduced by carefully controlling the growth conditions, the “intrinsic” FSS is still present even for an idea cylindrical dot, because semiconductor materials from which dots are commonly made have the zinc-blende structure and are thus not spatially isotropic. The zinc-blende structure has T_d symmetry, so even a cylindrically shaped, i.e., lens or cone, QD made of a zinc-blende semiconductor can only have a subgroup C_{2v} symmetry [17]. Since the interface between the dot material and the surrounding matrix material is not necessarily a reflection plane, the (atomistic) potentials are different along the [110] and $[1\bar{1}0]$ directions [17], leading to a natural, built-in intrinsic FSS [Fig. 1(b)]. Such atomistic effects are commonly missed by continuum models (such as the effective mass approximation and the few-band $k \cdot p$ method), which “see” only the macroscopic shape symmetry, rather than atomistic details [18]. However, recent atomistic calculations show that the intrinsic FSS is around several tens of μeV in the InAs/GaAs QDs [19].

Here we design a QD system with reduced FSS by using the microscopic understanding of the origins of the intrinsic FSS [19]. We recognize three factors here. First, atomic relaxation due to lattice size mismatch between the dot and matrix materials (e.g., InAs and GaAs, respectively, have a 7% mismatch) enhances the magnitude of both intrinsic and shape-asymmetry FSS [19]. Thus one could expect that the dot-matrix system with lower lattice mismatch should have smaller FSS. Second, a stronger confinement of the electron and hole in their respective potential wells will reduce the penetration of the respective wave functions into the matrix material, thus reducing their amplitude at the interface, where intrinsic asymmetry is present. Third, since the (atomistic) hole wave functions are more localized on the anion sites, having dot and matrix material with different anions (e.g., As vs P or N) will further reduce the amplitude of hole wave functions at the interface, thus reducing the intrinsic FSS.

Surprisingly, all three conditions can be met by retaining InAs as the dot material but replacing the commonly used GaAs matrix material by InP. The latter material has a smaller lattice mismatch with InAs (3% instead of 7% for GaAs) and manifests a different anion (P) with respect to the As atom in GaAs. To examine the extent to which the

InP matrix better confines the electron-hole wave function inside the InAs dot, we compare in Fig. 2 the strain-modified potential in an InAs dot surrounded by GaAs or InP. The dominant contribution to the electron-hole exchange energy comes from the overlap between the electron and hole wave functions. Since the electron wave function (e_0 in the inset in Fig. 2) is similar in both systems due to the light electron mass of InAs, the dimension of the electron-hole overlap is mainly determined by the hole wave function. As shown in Fig. 2, the (strained) hole confining potential for InAs/InP is 530 meV, much larger than that for InAs/GaAs (280 meV). Consequently, the hole wave function of the InAs/InP system (h_0 in the inset in Fig. 2) is indeed much more localized in the dot interior than is the case in the InAs/GaAs dot [20]. The reduced wave function amplitude at the interface, where the [110] vs $[1\bar{1}0]$ asymmetry is maximal, will then reduce the intrinsic FSS in InAs/InP.

To examine our design principles for reduced FSS at work, we carried out extensive calculations of the exciton energies and their FSS for 184 different dots in the InAs/InP and InAs/GaAs QDs. We have considered realistic sizes and geometries, including lens-shaped QDs (L1–L5), (truncated-)cone-shaped QDs (C1–C5), and elongated QDs (E1 and E2) (see Table I). We use an atomistic pseudopotential approach to describe the single-particle physics [20,21], and a configuration-interaction approach to describe the many-body interactions [22]. The methods were described in detail in Refs. [19–22]. For the configuration-interaction calculations, we use all possible Slater determinants constructed from the 12 lowest energy

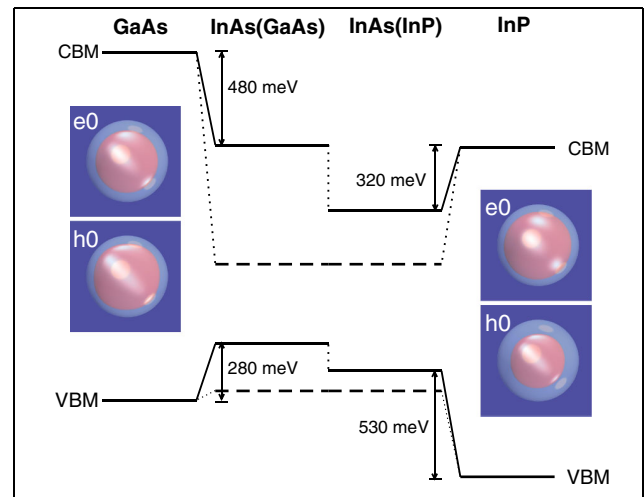


FIG. 2 (color online). Energy band offsets for the InAs/GaAs and InAs/InP QDs. The solid lines represent the strain-modified band offsets, whereas the dashed line is the unstrained conduction-band minimum (CBM) and valence-band maximum (VBM) for InAs. We show in the inset the first electron (e_0) and hole (h_0) wave functions of the lens-shaped InAs/GaAs and InAs/InP QDs, with base = 25 nm and height = 2.5 nm. The isosurface is chosen to enclose 95% of the total density.

TABLE I. Geometries of the QDs used in the calculations. D is the base diameter of the lens-shaped and (truncated-)cone-shaped dots, whereas h is the height of the dots. S is defined as $R_{[110]} \cdot R_{[1\bar{1}0]}$, where $R_{[110]}$ and $R_{[1\bar{1}0]}$ are the diameters of the (elongated) QDs along the $[110]$ and $[1\bar{1}0]$ direction, respectively.

	Shape	Size
L1	Lens	$D = 20$ nm, $h = 2.5$ – 5.5 nm
L2	Lens	$D = 25$ nm, $h = 2.5$ – 5.5 nm
L3	Lens	$h = 3$ nm, $D = 20$ – 25 nm
L4	Lens	$h = 4$ nm, $D = 20$ – 25 nm
L5	Lens	$h = 5$ nm, $D = 20$ – 25 nm
C1	Cone	$D = 20$ nm, $h = 2.5$ – 5.5 nm
C2	Cone	$D = 25$ nm, $h = 2.5$ – 5.5 nm
C3	Cone	$h = 3$ nm, $D = 20$ – 25 nm
C4	Cone	$h = 4$ nm, $D = 20$ – 25 nm
C5	Cone	$h = 5$ nm, $D = 20$ – 25 nm
E1	Elongated	$S = 20^2$ nm ² , $h = 4.5$ nm
E2	Elongated	$S = 25^2$ nm ² , $h = 4.5$ nm

electron and holes states (including spin), which converge very well with the results. Since the exciton and biexciton are nearly linearly polarized along the $[110]$ direction and the $[1\bar{1}0]$ direction [19], the FSS is defined as the energy splitting between the $[110]$ polarized exciton and $[1\bar{1}0]$ polarized exciton, i.e., $\Delta_{\text{FSS}} = E(X_{[110]}) - E(X_{[1\bar{1}0]})$.

Figure 3 shows the FSS in these two systems as a function of the excitonic energy [23]. The exciton energies of the (pure) InAs/GaAs QDs range from 0.95 to 1.12 eV, and the FSS scatters from -18 to 60 μeV , both in good agreement with experiments [8–12], which establishes credibility for the results of the InAs/InP dots. Figure 3 demonstrates that the intrinsic FSS of the InAs/InP QDs (-4 – 6 μeV) is about an order of magnitude smaller than that of the InAs/GaAs QDs. This system can therefore be used as an efficient entangled photon source. Furthermore, since the primary exciton wavelength of the InAs/InP QDs is around the 1.55 μm telecommunications wavelength [20,24,25], they are very promising for long distance quantum communication via optical fibers. In Refs. [24,25], the authors mentioned that the FSS of the few InAs/InP samples they measured have very small FSS, without any further discussions. Since it is well known that the FSS is a statistically distributed quantity, the small FSS these authors have obtained for just a few samples does not imply that for InAs/InP the statistical average of the FSS is intrinsically small, whereas for InAs/GaAs it is intrinsically large. This is what we discover in our work.

The FSSs of the InAs/GaAs and InAs/InP QDs are compared in Fig. 4 for different dot geometries given in Table I. Figures 4(a)–4(d) show the results for shape-symmetric dots (circular base), whereas Figs. 4(e) and 4(f) illustrate the effects of shape asymmetry (base with different radii lengths).

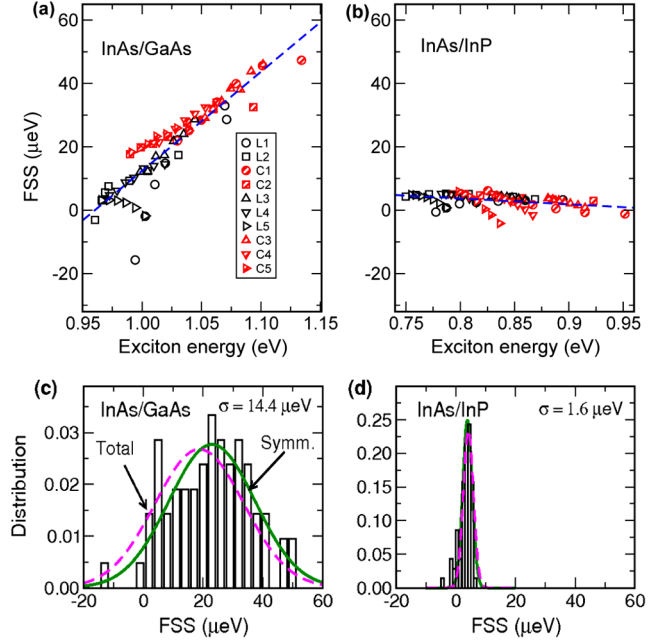


FIG. 3 (color online). The upper panel shows the FSS vs the exciton energy for (a) InAs/GaAs and (b) InAs/InP QDs. The lower panel shows the FSS distributions for (c) InAs/GaAs and (d) InAs/InP QDs. The solid lines are fitted by Gaussian functions for all shape-symmetric QDs, whereas the dashed lines represent the distributions of the FSS of total samples including also the asymmetric dots. σ is the standard deviation of the distribution.

Intrinsic FSS vs dot height.—For the InAs/GaAs dots, the FSSs decrease monotonically with increasing of the dot height. At about $h = 5$ nm, the FSS of the InAs/GaAs dot L1 is found to be zero. This is because, in the tall InAs/GaAs QDs, the holes are localized at the interface of the dot due to the strain effect [26], which reduces the electron-hole wave function overlap, leading to small FSS. However, it is not a good way to reduce the FSS by increasing the dot height for the InAs/GaAs QDs, because the photoluminescence (PL) intensity is also reduced with the deduction of the FSS due to the reducing of electron-hole overlap. The height effect of the FSS is less dramatic for the InAs/InP dots, and all FSSs are found to be extremely small (between -4 to 6 μeV). A zero FSS is also found for the L1 InAs/InP dots at height ~ 5.5 nm. Unlike in the InAs/GaAs dot, the holes are not localized on the interface in the InAs/InP QDs [20]; therefore, it would not suffer the problem of PL intensity suppression as in the tall InAs/GaAs dots.

Intrinsic FSS as a function of dot base size.—For flat InAs/GaAs QDs (L4 and C4), the FSS decrease monotonically with increasing of the base size. However, for the tall InAs/GaAs dot (L5), as we increase the base size, the FSS increases, because the hole is less localized on the interface [26], which increases the electron-hole overlap and thus the FSS. For InAs/InP dots, the FSSs increase slightly as we increase the base size for all dot geometries. The FSSs

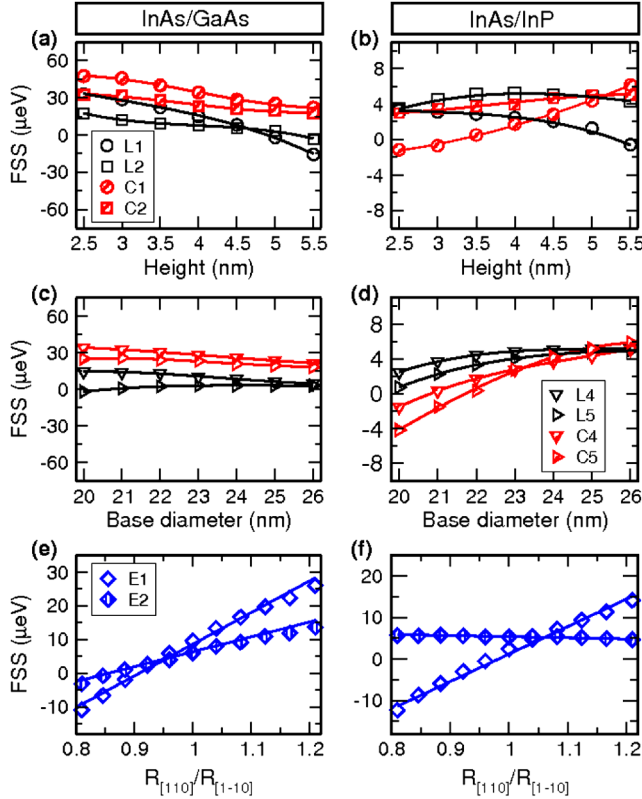


FIG. 4 (color online). Upper panel: The height dependence of the FSS for (a) InAs/GaAs and (b) InAs/InP QDs with different sizes and geometries (lens and cone). Middle panel: The base diameter dependence of the FSS for (c) InAs/GaAs and (d) InAs/InP QDs. Lower panel: The FSS as a function of the lateral aspect ratio of the elongated QDs in (e) InAs/GaAs and (f) InAs/InP QDs.

of the cone-shaped dots are similar to that of the lens-shaped dots.

Effect of shape asymmetry to FSS.—Figure 4(e) depicts the FSS of the InAs/GaAs QDs as functions of the lateral aspect ratio $R_{[110]}/R_{[1\bar{1}0]}$, whereas Fig. 4(f) shows the results for the InAs/InP QDs, for two fixed dot volume and height. For InAs/GaAs QDs, we see that, as we increase the asymmetric ratio, the FSS increase dramatically from -11 to $26 \mu\text{eV}$. For the InAs/InP QDs, we found that, for the smaller QDs, the FSS depends strongly on the shape asymmetry of QDs (from -12 to $14 \mu\text{eV}$), whereas for the larger dot, the FSS only weakly dependent on the shape asymmetry.

Statistical distribution of FSS vs sizes and shapes.—The statistical distributions of FSS for the two types of dots are plotted in Figs. 3(c) and 3(d), respectively. The solid lines represent the distributions of the intrinsic FSS of cylindrical QDs fitted by Gaussian functions, and the dashed line represent the distributions of the FSS of total samples including also the asymmetric dots. As we see, including the asymmetric dots does not change the FSS distribution much. The mean value of the FSS of the InAs/GaAs dots is $23 \mu\text{eV}$, with a standard deviation of $14.4 \mu\text{eV}$, whereas

the average FSS of the InAs/InP dots is $3.5 \mu\text{eV}$ and the standard deviation is only $1.6 \mu\text{eV}$. The FSS of the InAs/InP dots can be further reduced by controlling the growth condition. For example, for the “small” InAs, InP lattice mismatch, one may try to grow a quantum disk, which has higher D_{2d} symmetry and thus (almost) zero FSS. Nevertheless, it is much easier to obtain the InAs/InP QDs with nearly zero FSS than the InAs/GaAs dots.

In conclusion, we have shown that the *intrinsic* FSSs of the InAs/InP dots are (statistically) about an order of magnitude smaller than that of the InAs/GaAs dots. The InAs/InP QDs have additional advantages because the emission photon wavelength is around $1.55 \mu\text{m}$ and is far away from the wetting layer background emissions. Combining these advantages, one can expect that the InAs/InP QDs can play a crucial role in the quantum information applications, as a new generation of “on-demand” entangled photon source.

L. H. acknowledges the support from the CNFR Program 2006CB921900 and NSFC (Grant No. 10674124). A. Z. acknowledges support from U.S. DOE-SC-BES-DMS, LAB-17 initiative, under Contract No. DE-AC36-99GO10337 to NREL.

*Corresponding author.
helx@ustc.edu.cn

- [1] A. Aspect *et al.*, Phys. Rev. Lett. **49**, 91 (1982).
- [2] Z. Y. Ou and L. Mandel, Phys. Rev. Lett. **61**, 50 (1988).
- [3] T. Jennewein *et al.*, Phys. Rev. Lett. **88**, 017903 (2001).
- [4] N. Gisin *et al.*, Rev. Mod. Phys. **74**, 145 (2002).
- [5] J. I. Cirac *et al.*, Phys. Rev. A **59**, 4249 (1999).
- [6] O. Benson *et al.*, Phys. Rev. Lett. **84**, 2513 (2000).
- [7] R. M. Stevenson *et al.*, Nature (London) **439**, 179 (2006).
- [8] R. J. Young *et al.*, Phys. Rev. B **72**, 113305 (2005).
- [9] A. Högele *et al.*, Phys. Rev. Lett. **93**, 217401 (2004).
- [10] A. I. Tartakovskii *et al.*, Phys. Rev. B **70**, 193303 (2004).
- [11] N. Akopian *et al.*, Phys. Rev. Lett. **96**, 130501 (2006).
- [12] R. Seguin *et al.*, Phys. Rev. Lett. **95**, 257402 (2005).
- [13] R. J. Young *et al.*, New J. Phys. **8**, 29 (2006).
- [14] M. Bayer *et al.*, Phys. Rev. Lett. **82**, 1748 (1999).
- [15] G. Dresselhaus, Phys. Rev. **100**, 580 (1955).
- [16] Y. A. Bychkov *et al.*, J. Phys. C **17**, 6039 (1984).
- [17] G. Bester *et al.*, Phys. Rev. B **71**, 045318 (2005).
- [18] A. Zunger, Phys. Status Solidi B **224**, 727 (2001).
- [19] G. Bester *et al.*, Phys. Rev. B **67**, 161306(R) (2003).
- [20] M. Gong *et al.*, Phys. Rev. B **77**, 045326 (2008).
- [21] A. J. Williamson *et al.*, Phys. Rev. B **62**, 12963 (2000).
- [22] A. Franceschetti *et al.*, Phys. Rev. B **60**, 1819 (1999).
- [23] In the present work, we show the *intrinsic* FSS for selected geometries, which should not be directly compared to the trend of the FSS vs exciton energy for a particular thermal annealing process (e.g., Ref. [8]), because the structure and composition of the QDs change dramatically during the thermal annealing.
- [24] N. I. Cade *et al.*, Appl. Phys. Lett. **89**, 181113 (2006).
- [25] D. Kim *et al.*, Appl. Phys. Lett. **87**, 212105 (2005).
- [26] L. He *et al.*, Phys. Rev. B **70**, 235316 (2004).